Role of Dielectric Drag in Polaron Mobility in Lead Halide Perovskites

Mischa Bonn[1,*,†], Kiyoshi Miyata[2,*,†], Euan Hendry[3], X.-Y. Zhu[2,*]

[1.] Max Planck Institute for Polymer Research, Ackermannweg 10, 55128 Mainz, Germany

[2.] Department of Chemistry, Columbia University, New York, NY 10027, USA

[3.] Department of Physics & Astronomy, University of Exeter, Exeter EX4 4QJ, UK

ABSTRACT. Hybrid organic-inorganic lead-halide perovskites (HOIPs) have attracted much attention because of their remarkable charge carrier properties, including defect tolerance and low recombination rates that lead to long carrier lifetimes and diffusion lengths. These properties have been attributed to the efficient screening of charge carriers via polaron formation in the highly polar and dynamic environment of an HOIP. Polaron formation explains, at least in part, the moderate charge carrier mobility. However, measured mobilities in these materials (typically 10s-100 cm^2/Vs) are still lower than predicted from standard polaron theory. Here we discuss a factor that has been previously overlooked and can potentially account for the discrepancy between measured carrier mobility and that calculated using polaron theory: the effect of dielectric drag. An HOIP can be viewed as consisting of two sub-lattices: an inorganic lead halide sub-lattice responsible for the band structure and a disordered organic cation sub-lattice which is more weakly coupled to the electronic degrees of freedom. While optical phonon modes of the lead halide sub-lattice are mainly responsible for polaron formation, slower orientational relaxation of surrounding dipoles adds a dielectric drag to the moving charge. We discuss the role of this dielectric drag based on the measured dielectric function in the GHz – THz frequency range and how we can understand the unique carrier physics in HOIPs in view of its crystal-liquid duality.

[*]To whom correspondence should be addressed.
[†] These authors contributed equally
MB: bonn@mpip-mainz.mpg.de; KM: km3097@columbia.edu; XYZ: xyzhu@columbia.edu

1. Introduction

Since the discovery of their potential photovoltaic applications in 2009 by Kojima et al.,[1] the optoelectronic properties of hybrid organic-inorganic lead-halide perovskites (HOIPs) have been explored extensively with great success.[2–7] In particular, long carrier lifetimes, long carrier diffusion lengths, and exceptional defect-tolerance are beneficial to many optoelectronic applications.[8–13] Even though the initial success had focused on HOIPs, their all-inorganic counterparts have also attracted growing attention. A large body of work has been devoted to understanding "why" lead halide perovskites work so well, but a unified understanding at the microscopic level, is still lacking. These exceptional properties may be related to the softness and dynamic disorder of the ionic lattice consisting of a sub-lattice of corner-sharing PbX_6^{3-} (X = I, Br, or Cl) octahedrals with a stoichiometry of PbX_3^-, and a sub-lattice of A^+ cations.[14] The A^+ ion can be either organic cations, $CH_3NH_3^+$ (MA) or $NH_2(CH)NH_2^+$ (FA), in an HOIP or inorganic cations (Cs^+ or Rb^+). The cage-structure, along with the high polarizability of Pb and its less-directional bonding than transition metals, results in exceptional flexibility and dynamic disorder on fs-ps timescale.[15,16] The latter leads to electronic energy fluctuation of the conduction band minimum (CBM) and the valance band maximum (VBM) by 10s-100 meV.[17,18] Although the A^+ cations are not directly involved in the band structure, they further contribute to the dynamic disorder of electronic structure by rattling and/or reorienting in the cuboctahedral voids. In both HOIPs and its all-inorganic counterparts, the relative position of the A^+ with respect to the anionic PbX_3^- cage can be represented by a dipole moment.[19] This is in addition to the permanent dipole moment of the molecular A^+ cation in an HOIP. All those structural properties result in rather "liquid-like" structural flexibility as detected by various scattering and spectroscopic measurements.[16,20–31] Mechanical measurements also reveal a soft lattice, independent of cation type, with Young's moduli of lead halide perovskite ~10x lower than those in Si or GaAs.[32] A central question here is how optoelectronic properties are related to such unique structural characteristics.

Charge carriers in a soft and ionic lattice, as is the case for lead halide perovskites, must form polarons.[33–35] Miyata et al. directly probed the ultrafast phonon response to charge injection in $MAPbBr_3$ and $CsPbBr_3$ using femtosecond optical Kerr effect spectroscopy, in conjunction with first principles calculations.[31] They found that a polaron forms predominantly from the deformation of the $PbBr_3^-$ frameworks, irrespective of the cation type, with polaron formation

time constants of 0.3 ps in $CH_3NH_3PbBr_3$ and 0.7 ps in $CsPbBr_3$. The dominance of charge carrier coupling to the deformation modes of the PbX_3^- framework has also been confirmed in the two-dimensional electronic spectroscopy study of Fleming and coworkers [36] and in the THz pump – visible probe experiments of Bonn and coworkers[37] on $CH_3NH_3PbI_3$ thin films.

Zhu and Podzorov hypothesized that the Coulomb screening through large polaron formation might explain the remarkable properties of lead halide perovskites.[38] As a result of screening, the scattering of carriers with other carriers and charged defects is reduced, thus contributing to low recombination rate[11] and defect tolerance.[39–41] The screening also reduces further cooling of dressed carriers, thus contributing to long-lived energetic carriers in HOIPs.[29,42] The polaron picture provides a better explanation of charge carrier mobility: measured mobilities in lead halide perovskites are in qualitative agreement with calculations based on the large polaron model.[27,31] Moreover, the large polaron model explains qualitatively the band-like transport characterized by a decrease of mobility with increasing temperature.[38] Here, we provide our understanding of carrier mobility in HOIPs and point out a potential factor which has been overlooked: an additional reduction of charge carrier mobility from dielectric drag due to reorientational motions of dipoles.

2. Mobility from the Feynman polaron model

Electronic structure calculations of lead halide perovskites show small effective electron/hole masses of 0.1-0.2 m_e (m_e: bare electron mass),[43–45] which corresponds to mobility of the order of 10^3 cm^2/Vs from prototypical band theory. However, experimental mobilities have been reported in the 10-100 cm^2/Vs range,[46] including those in single crystals.[9,10,13,47,48] These lower mobilities are expected from the polaron model established by Feynman[35,49] and Osaka[50]. This model covers the polaron physics from the weak to the strong coupling regime seamlessly and has been successfully applied to the analysis of a broad range of electronic materials, e.g., TiO_2[51] and $Bi_{12}SiO_{20}$[52]. In this model, the polaron is characterized by four parameters: the band effective mass (m), the longitudinal optical (LO) phonon frequency (ω_{LO}) and the dielectric constant at higher and lower frequency than that of LO phonons, referred to here as optical (ε_{opt}) and static (ε_s) dielectric constants, respectively. These parameters determine the Frohlich electron-phonon coupling parameter,[33] $\alpha_{e\text{-}ph}$, defined by:

$$\alpha_{\mathrm{e-ph}} \equiv \frac{e^2}{\hbar}\left(\frac{1}{\varepsilon_{opt}} - \frac{1}{\varepsilon_s}\right)\sqrt{\frac{m}{2\hbar\omega_{\mathrm{LO}}}} \qquad (1)$$

where e is the charge of an electron and $\hbar$ is the reduced Planck constant. The value of $\alpha_{\text{e-ph}}$ determines whether a polaron is in the large-intermediate polaron ($\alpha_{\text{e-ph}} < 6$) or a small polaron ($\alpha_{\text{e-ph}} >> 6$) regime, where large/small refers to the polaron radius.

Using measurements of far-IR absorption spectra, Sendner et al. have calculated the properties of Feynman polarons in $MAPbX_3$ (X=Cl, Br, I) and confirmed the polarons in lead halide perovskites are in the large-to-intermediate regime.[27] Miyata et al. analyzed $MAPbBr_3$ and $CsPbBr_3$ with the Feynman polaron model and reported large polaron sizes and mobilities in conjunction with ab initio calculations.[31] The calculated $\alpha_{\text{e-ph}}$ values, polaron radii (ρ), and mobilities (μ) from these two reports are shown in Table 1. These calculations gave the Frohlich coupling constants in the range of 1 - 3, polaron radii of 2.5 – 5.1 nm, and electron/hole mobilities of 40 - 200 cm^2/Vs, all consistently in the regime of intermediate-to-large polarons. Overall, the calculated mobilities are higher than experimental values by more than a factor of two for the HOIPs.[46] This might imply another intrinsic reduction in mobility which is not taken into account in the present analysis.

Table 1: Key polaron parameters of lead halide perovskites calculated from the Feynman-Osaka theory at 300 K:[27,31] Frohlich couplings ($\alpha_{\text{e-ph}}$), large polaron sizes (ρ), and room temperature mobilities (μ). The labels –e, –h, and -<e,h> correspond to values for electron, hole, and average e/h, respectively.

Material	$\alpha_{\text{e-ph}}$	ρ [nm]	μ [cm^2/Vs]	Ref.
$MAPbI_3$ - <e, h>	1.72	5.1	197	Sendner et al. [27]
$MAPbBr_3$ - <e, h>	1.69	4.3	158	Sendner et al. [27]
$MAPbCl_3$ - <e, h>	2.17	2.7	58	Sendner et al. [27]
$MAPbBr_3$ - h	1.87	3.1	79	Miyata et al. [31]
$MAPbBr_3$ - e	1.54	4.2	150	Miyata et al. [31]
$CsPbBr_3$ - h	2.76	2.5	41	Miyata et al. [31]
$CsPbBr_3$ - e	2.64	2.7	48	Miyata et al. [31]

3. Temperature dependence

Much insight into the polarons can be obtained from the temperature dependence in charge carrier mobilities and recombination rates. These dependences can reveal whether the mechanism of transport is coherent band-like or incoherent hopping type.[34] The large-intermediate polaron, with radius larger than unit cell dimension, is characterized by coherent band transport with mobility decreasing with increasing temperature, $d\mu/dT < 0$, as is the case in lead halide perovskites.[38] This is in contrast to the transport of a small polaron, with radius smaller than unit cell dimension, which is characterized by thermally activated transport, $d\mu/dT > 0$.[34] For an intermediate-large polaron, the quantitative temperature dependence in mobility reflects the origin of carrier scattering.

Temperature-dependent transport and spectroscopy measurements in HOIPs have established scaling relationships of $\mu \propto T^{-\gamma}$, with γ varying in the range of 0.5 to 1.7,[48,53–56] consistent with $d\mu/dT < 0$ in band transport of large polarons. Interestingly, the commonly observed γ values of approximately 1.5 from various experiments, including Hall-effect measurement on single crystal $MAPbBr_3$ in the cubic phase,[48] and microwave, GHz, and THz spectroscopies on polycrystalline $MAPbI_3$,[53–56] are in agreement with the prediction of Bardeen and Shockley for acoustic phonon scattering in nonpolar semiconductors.[57] However, this agreement could be incidental as theoretical analysis of acoustic phonon scattering in HOIPs yields charge carrier mobilities more than one order of magnitude higher than experimental values.[58–61] Instead, theoretical analysis[62] and temperature-dependent photoluminescence (PL) measurements[63,64] suggest that longitudinal optical (LO) phonons should be the dominant origin of e-phonon scattering. It is interesting to note that, due to the low energies of LO phonons in these materials (see below),

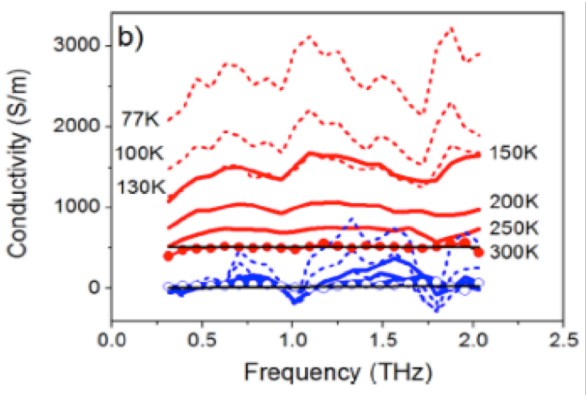

Fig. 1. Temperature dependence of terahertz spectra. Complex-valued photoconductivity (real part in red, and imaginary part in blue) in $MAPbI_xCl_{3-x}$ thin film as a function of temperature (between 300 and 77 K) measured at 6 ps after photoexcitation. Solid and dashed lines represent the response for the tetragonal and orthorhombic phases, respectively. Black solid lines represent best fits to the Drude model. From Karakus et al. ref. [55].

one does not expect the exponential temperature dependence of scattering from LO phonons that is typically observed in ionic crystals [51].

A temperature-dependent measurement also allows one to assess the role of molecular dipole rotation in HOIP across the phase transitions, from the low-temperature orthorhombic phase where the molecular dipole is frozen, to the intermediate tetragonal phase and the high-temperature cubic phase where the molecular dipole attains increasing rotational freedom with temperature. Karakus et al. measured temperature dependent photo excited terahertz conductivity of highly crystalline $MAPbI_3$ thin films over a temperature range of 77 – 300 K, Fig. 1.[55] They observed a Drude-like response which manifests itself in the absence of negative imaginary part over a wide terahertz range. Note that even across the phase transition from the tetragonal to the orthorhombic phase, the Drude-like response was observed. From the fitting based on the Drude model, they successfully extracted the frequency of momentum scattering in the film as a function of temperature (4 fs^{-1} at 300 K, 13 fs^{-1} at 150 K). They also reported the scaling of $\mu \propto T^{-\gamma}$, with the power γ = 1.2 in the orthorhombic phase and γ = 1.5 in the tetragonal phase. This change in γ across the phase boundary suggests that dipole rotation, from a frozen geometry to hindered rotation, might play a role in the scattering mechanisms. Yi et al. examined Hall mobility in $MAPbBr_3$ single crystals as a function of temperature, Fig. 2.[48] They observed temperature dependent Hall mobility following the scaling law of $\mu \propto T^{-\gamma}$, with γ = 0.5 ±0.1 in the tetragonal phase and γ = 1.4 ±0.1 in the cubic phase. In addition to this change in γ values, they also observed an abrupt decrease (by a factor of two) in Hall mobility across the tetragonal-cubic transition. Such changes across the phase boundary again suggest the role of molecular dipoles, from hindered to nearly-free rotation, in the scattering mechanism.

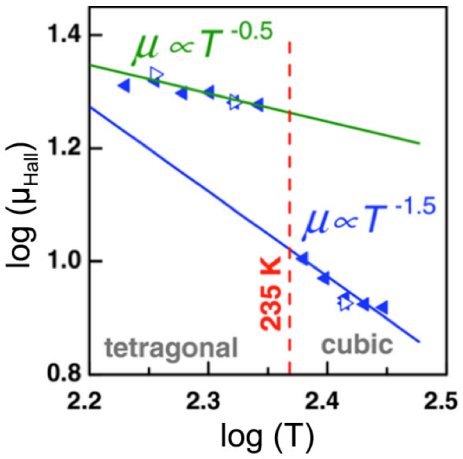

Fig. 2. Temperature dependence of Hall mobility in $MAPbBr_3$ single crystal. The fits to μ_{Hall} ($cm^2V^{-1}s^{-1}$) $\propto T$ (K)$^{-\gamma}$ give γ = 0.5±0.1 in the tetragonal and γ = 1.4±0.1 in the cubic phases. From Yi et al. ref. [48].

Despite its qualitative success in explaining the low mobility, the Feynman polaron theory seems to overestimate the experimental charge carrier mobilities in HOIPs[46] by at least a factor of ~two, as detailed in table 1.[27,31] Moreover, the magnitudes of the temperature dependent changes also disagree: while the temperature dependent THz measurement in Fig. 1 suggests a decrease in scattering time from 13 fs to 4 fs – i.e. a threefold decrease – when temperature is increased from 150 K to 300 K,[55] the Feynman polaron theory predicts the scattering time to decrease by a factor of 1.5 over the same temperature range – from 150 fs to 100 fs.[65] Thus, the absolute scattering rate is underestimated in theory. Moreover, the polaron model[27] predicts a rather weak temperature dependence of the mobility of $\gamma = 0.6$, which matches the observation of Hall mobility in $MAPbBr_3$ in the tetragonal phase,[48] but does not agree with the $\gamma = 1.4$-1.6 for $MAPbI_3$ or for $MAPbBr_3$ in the cubic phase.[48,54–56] Filippetti et al. found $\gamma = 1.5$ dependence in their ab initio calculation,[62] but the distinct temperature dependence in the different phases still cannot be fully explained.

4. The unusual dielectric function

HOIPs possess unusual dielectric functions in the THz to sub-THz range.[66,67] In a conventional inorganic semiconductor, lattice vibrations including transverse optical (TO) phonons in the ~1-10 THz region contribute to the dielectric function (ε) and increases Re(ε) by a few to a few 10s of percent from the high-frequency electronic response (~100s THz).[68] An HOIP is distinctively different, as illustrate for $MAPbI_3$ in the tetragonal phase: (1) In the high frequency region ($\nu \geq 10$ THz), the real part of the dielectric function, $\varepsilon_H \sim 4$, is dominated by the electronic response, with a small contribution from intramolecular vibrations (10-100 THz); (2) In the intermediate frequency range, $\nu \leq \sim 1$ THz, the activation of TO phonons attributed to PbX_3^- deformations increases Re(ε) by nearly one order of magnitude to $\varepsilon_M \sim 35$; (3) Further decreasing the frequency to $\nu \leq \sim 10$ GHz activates nearly free rotation of the molecular dipoles and the corresponding Debye relaxation increases Re(ε) by another factor of ~2 to $\varepsilon_L \sim 80$. At even lower frequencies (< GHz), ion migration can affect the response. Overall, the response is rather unusual for a crystal and resembles that observed in a typical polar liquid where the dielectric response in the THz and sub-THz region is dominated by diffusive molecular rotations.[69,70] In equation (1), the two dielectric constants, ε_{opt} and ε_s, would normally

correspond to ε_H and ε_M in Fig. 3. While the LO phonons at ~1-2 THz in Fig. 3 attributed to distortions of the PbX_3^- sub-lattice are strongly coupled to charge carriers, leading to large polaron formation and the major lowering of charge carrier mobility,[27,31,36,37] the Feynman polaron model does not take into account the lower frequency molecular dipole rotations represented by the second step at ~10 GHz where Re(ε) is further increased from ε_M to ε_L. Although the molecular dipole motions are indirectly coupled to the electronic degrees of freedom, they may further slowdown charge carrier motion in the form of "dielectric drag", as we elaborate below. A similar argument has been made by Anusca et al., who proposed that such a dielectric response results in a "hyperpolaron", which is formed by additional screening of a Fröhlich polaron by the rotation motion of dipolar MA^+ cations.[67]

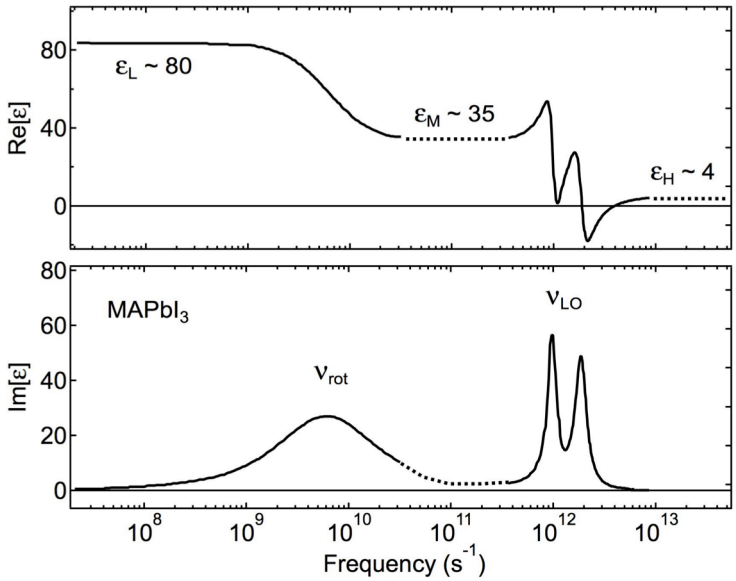

Fig. 3. Real (top) and imaginary (bottom) part of the dielectric functions in tetragonal phase (solid) of $MAPbI_3$ in the region of 10^7 - 10^{11} Hz at 210 K (left) where the MA^+ rotational relaxation response is included,[67] and in the region of 10^{11} - 10^{13} Hz at 300 K (right) where polar phonons of mainly the PbI_3^- sub-lattice dominate.[27] Dot lines are to guide the eye.

5. The possible role of dielectric drag

Dielectric drag is a well-developed concept for charge transport in solutions.[71,72] When a charge or ion is introduced into a polar solvent, the solvent will respond through the rotational relaxation of its molecular dipoles. Such solvation affects not only the total energy stabilization but also the ion conductivity because an ion needs to drag along the rotational motions of surrounding rotatable dipoles.[71,72] This phenomenon is called *dielectric drag*. Since the dielectric function of an HOIP resembles those of polar liquids (Fig. 3), we propose that charge carrier mobility is determined by not only large polaron formation due to strong coupling to the LO

phonons, but also dielectric drag due to rotational relaxation of the disordered molecular dipoles. There has been much confusion on these two types of lattice motions in recent literature on lead halide perovskites, but the underlying physical mechanism are qualitatively different. The standard definitions of optical ($\varepsilon_{\mathrm{opt}}$) and static ($\varepsilon_{\mathrm{s}}$) dielectric constants are different for polaron formation and solvation. In the Feynman polaron model, $\varepsilon_{\mathrm{opt}}$ and ε_{S} refer to the value of Re(ε) above and below the ν_{LO}, respectively. However, in models for dielectric drag (discussed below), the relevant region of the dielectric function bounds ν_{rot}, the frequency of molecular dipole rotation. It is therefore necessary to distinguish at least three relevant values for the dielectric permittivity to treat both physics on the same footing. Here we describe these as low (ε_L), medium (ε_M), and high frequency dielctric constants (ε_H). Polaron formation is related to the difference in ε_H and ε_M, while solvation is characterized by ε_M and ε_L.

To examine the significance of dielectric drag, here we start from the simplest equation of the motion of carriers, consistent with Drude-type spectral response previously observed over a large temperature range in THz pump-probe spectroscopy.[55] The polaron experiences friction from dielectric drag (F_{DD}) in addition to friction from the Drude model (F_D). The equation of motion of the carriers under constant electric field, *E*, can be described as:

$$m\frac{\mathrm{d}v}{\mathrm{d}t} = qE - F_D - F_{DD} \quad (2)$$

$$F_D = \frac{mv}{\tau} \quad (2a)$$

$$F_{DD} = \zeta v \quad (2b)$$

where m is the effective mass of the carrier (polaron mass); q is the carrier charge; v is the velocity of the carrier; τ is the polaron momentum scattering time; and ζ is the friction caused by dielectric drag. To compare the relative significance of ζ with Drude scattering, we transform the above equation to

$$m\frac{\mathrm{d}v}{\mathrm{d}t} = qE - mv\left[\frac{1}{\tau} + \frac{\zeta}{m}\right]. \quad (3)$$

which enables us to compare the two effects in the unit of scattering rate (s^{-1}). According to the description of ζ established by Zwanzig in the continuum dielectric model,[72]

$$\zeta = \frac{3}{4}\left(\frac{q^2}{a^3}\right)\left[\frac{\epsilon_L - \epsilon_M}{\epsilon_L(2\epsilon_L + 1)}\right]\tau_1 \quad (4)$$

where a is the ion radius; τ_1 is a characteristic time of Debye relaxation. Here, we employed the case of slip boundary condition because the boundary of a polaron should not be as well-defined as that of an ion and we should expect less friction. Unlike the initial description by Zwanzig, Heitele pointed out that the characteristic time (τ_1) is the LO component of Debye relaxation time described by $\tau_1 = (\varepsilon_M/\varepsilon_L)\tau_D$ where τ_D is a Debye relaxation time.[73]

Using this set of equations, we examine the case of $MAPbI_3$. From terahertz photoconductivity measurements, the room temperature scattering rate in the film has been inferred from the Drude model to be k_{tot} = 0.25 fs^{-1} with m=0.25 m_e.[55] Within the framework presented here, this overall scattering rate k_{tot} contains contributions from both polaron scattering and dielectric drag: $k_{tot} = 1/\tau + \zeta/m$. Estimating the contribution from dielectric drag, ζ/m -, requires knowledge of four parameters: a, ε_M, ε_L and τ_D. We take a as large polaron radius of 5.1 nm.[27] We take ε_L= 80 and ε_M= 35 to approximate the room temperature dielectric constant in the GHz-THz range.[67] Dipole rotation time has been directly measured by anisotropy decay in two-dimensional infrared spectroscopy,[74] which report the second order reorientation time, $\tau^{(2)}$=3 ps, corresponding to a Debye relaxation time $\tau_D = 3\tau^{(2)} = 9$ ps.[75] While this constitutes a very crude estimate, inserting these values into equation (4) gives an effective scattering rate of $\frac{\zeta}{m}$ = 0.9 fs^{-1}. We must realize that this calculation over-estimates the effective scattering rate, as it assumes a complete and static response of the dipolar MA^+ cations to the charge. In reality, an electron/hole cannot be considered as a static charge, since mobilities in perovskite materials are orders of magnitude higher than those of solvated ions or charges. To treat this properly, it is well-known that the wavevector dependence of dielectric functions should be taken into account for a truly quantitative understanding in the case of solvation dynamics.[76–78] To correct for this overestimation, we consider the relative velocities of MA^+ dipole rotation and charge carrier transport. The MA^+ dipole reorientation time (jump-like motion) of 3 ps over π/2 corresponds to an angular rate of ~0.52 rad/ps, or v_F = ~3 nm/ps for an MA^+ cation in the first "solvation shell" at ~5 nm from the center of a large polaron. Dielectric drag affects both the thermal velocity and the drift velocity of the carriers. The thermal velocity of an electron or hole at room temperature is $v_e = (2k_BT/m)^{1/2}$ = 200 nm/ps, where the effective

polaron mass is set at 0.25 m_e. We do not know the exact functional relationship between scattering rate and relative velocity. To the zeroth order approximation, we assume a linear scaling and this leads to the reduction of ~67x of the calculated scattering rate from equation (4). Note that the "jump-like" reorientational motion is not the fastest motion and the "wobbling-in-a-cone" motion of MA^+ is the nanoscopic cage is 10 times faster, with a time constant of ~0.3 ps.[74] If the wobbling motion dominates the polarization response, the calculated scattering rate from equation (4) should likely be reduced by one-order-of-magnitude, to $\frac{\zeta}{m}$ ~ 0.09 fs^{-1}. This is ~1/3 of the overall friction rate, k_{tot} = 0.25 fs^{-1}.

The above discussion suggests an experimental approach to probe the dielectric drag quantitatively using the drift velocity. The drift velocity of charge carriers can be controlled by an electric field, i.e., bias voltage. As an example, for a 200 nm thick thin film and a carrier mobility of 100 $cm^2V^{-1}s^{-1}$, the drift velocity increases from 10^2 nm/ps to 10^3 nm/ps as the bias voltage increases from 2 V to 20 V. In the regime, the drift velocity can surpass the thermal velocity and an increase in drift velocity should decrease the relative contribution of dielectric drag to total scattering rate.

Another limitation to the equation (4) comes from the fact that solvation of large polarons in the rather unique environment possessing crystal-liquid duality necessitates the treatment of a *delocalized* charge. While ions are slow and rigid, normally giving rise to hydrostatic friction, large polarons are relatively light and fast moving, and should be regarded as electron clouds with less well-defined boundary. We also note that the radius of the solvation shell is likely larger than the radius of the polaron (typically ~5 nm in these materials). Therefore the effect might only be quantified in a quantum dynamics calculation with large unit cells, a challenge to current computational software and hardware. It is tempting to predict that dielectric drag plus large polaron formation may solve the enigma in the mobility and its temperature dependence in HOIPs, but more sophisticated theories beyond the equation 4 at the static limit is needed. Importantly, Ma and Wang recently demonstrated that carrier localization could happen, mediated by the random orientation of molecular dipoles.[79] They also made a connection between dipole rotation and the temperature dependence of the mobility.[80] The approach of Wang and Ma is related to solvation in our discussion of dielectric drag, but their neglect of polaron formation from the PbX_3^- sub-lattice is debatable. High-quality dielectric function

measurements in the range of GHz-THz over a broad temperature range are also necessary to capture dielectric response due to dipole reorientation in detail, and to shed light on the interesting issue experimentally.

Summary and Outlook

In this perspective, we introduce a potentially important concept to the understanding of charge carrier mobility in lead halide perovskites: the effect of dielectric drag. The dielectric drag might further clarify the physics behind carrier motion in HOIPs, including possible overestimation of mobility from the standard Feynman polaron theory and the temperature dependences in different phases where the rotational motion of molecular dipoles are most affected. The idea stems from the unique dielectric structure containing both solid-like phonon response mainly from the ionic lead-halide sub-lattice and rather liquid-like response from the rotational relaxation of dipoles in the voids of PbX_3^- octahedrals. We emphasize that the physical origins of polaron formation and solvation are fundamentally different: polaron formation is due to coupling with LO phonon *oscillation* (1-10 THz), while solvation mainly originates from rotational *relaxation* (<1 THz) of disordered dipoles. This is the reason we treated these two effects separately. We estimated the significance of dielectric drag from the simplest continuum model and show it could be a significant factor limiting mobility of charge carriers in HOIPs. The concept of the coexistence of polaron formation and dielectric solvation is likely general in material systems featuring crystal-liquid duality, such as carrier dynamics in phonon-glass electron-crystal or semiconductor/liquid interface. Finally, we point out that, while the above discussions focus on HOIPs, the same arguments may apply to their all-inorganic counterparts. Large polaron formation is known to be dominated by deformation of the PbX_3^- sub-lattice, irrespective of the cation type.[27,31,36,37] The subsequent motion of the large polaron may also experience dielectric drag due to slower dielectric relaxation of dipoles resulting the rattling of the A^+ with respect to the anionic PbX_3^- cage.[19]

Acknowledgements

We thank Prof. X. Roy, Dr. Johannes Hunger, Dr. Jarvist Frost, Prof. Shaul Mukamel, Prof.

Casey Hynes, and Prof. Louis Brus for insightful discussions. XYZ thanks Profs. Song Jin, Vitaly Podzorov and Filippo De Angelis for fruitful collaborations and his group, particularly Dr. Daniel Niesner, Dr. Xiaoxi Wu, Dr. Haiming Zhu, Dr. M. Tuan Trinh, Mr. Jue Wang, and Ms. Prakriti Joshi, for the experimental work which precipitated the ideas presented here. XYZ acknowledges US Department of Energy, Office of Science - Basic Energy Sciences, Grant ER46980 for support during the writing of this perspective. KM acknowledges JSPS for financial supports.

References

(1) Kojima, A.; Teshima, K.; Shirai, Y.; Miyasaka, T. Organometal Halide Perovskites as Visible-Light Sensitizers for Photovoltaic Cells. *J. Am. Chem. Soc.* **2009**, *131* (17), 6050–6051.

(2) Zhang, W.; Eperon, G. E.; Snaith, H. J. Metal Halide Perovskites for Energy Applications. *Nat. Energy* **2016**, *1*, 16048.

(3) *Organic-Inorganic Halide Perovskite Photovoltaics*; Park, N.-G., Miyasaka, T., Grätzel, M., Eds.; Springer: Switzerland, 2016.

(4) Veldhuis, S. A.; Boix, P. P.; Yantara, N.; Li, M.; Sum, T. C.; Mathews, N.; Mhaisalkar, S. G. Perovskite Materials for Light-Emitting Diodes and Lasers. *Adv. Mater.* **2016**, *28* (32), 6804–6834.

(5) Sutherland, B. R.; Sargent, E. H. Perovskite Photonic Sources. *Nat. Photonics* **2016**, *10* (5), 295–302.

(6) Manser, J. S.; Christians, J. A.; Kamat, P. V. Intriguing Optoelectronic Properties of Metal Halide Perovskites. *Chem. Rev.* **2016**, *116* (21), 12956–13008.

(7) Brenner, T. M.; Egger, D. a.; Kronik, L.; Hodes, G.; Cahen, D. Hybrid Organic—inorganic Perovskites: Low-Cost Semiconductors with Intriguing Charge-Transport Properties. *Nat. Rev. Mater.* **2016**, *1* (1), 15007.

(8) Xing, G.; Mathews, N.; Sun, S.; Lim, S. S.; Lam, Y. M.; Grätzel, M.; Mhaisalkar, S.; Sum, T. C. Long-Range Balanced Electron- and Hole-Transport Lengths in Organic-Inorganic CH3NH3PbI3. *Science* **2013**, *342* (6156), 344–347.

(9) Dong, Q.; Fang, Y.; Shao, Y.; Mulligan, P.; Qiu, J.; Cao, L.; Huang, J. Electron-Hole Diffusion Lengths > 175 Um in Solution-Grown CH3NH3PbI3 Single Crystals. *Science* **2015**, *347* (6225), 967–970.

(10) Shi, D.; Adinolfi, V.; Comin, R.; Yuan, M.; Alarousu, E.; Buin, A.; Chen, Y.; Hoogland, S.; Rothenberger, A.; Katsiev, K.; Losovyj, Y.; Zhang, X.; Dowben, P. a; Mohammed, O. F.; Sargent, E. H.; Bakr, O. M. Low Trap-State Density and Long Carrier Diffusion in Organolead Trihalide Perovskite Single Crystals. *Science* **2015**, *347* (6221), 519–522.

(11) Herz, L. M. Charge-Carrier Dynamics in Organic-Inorganic Metal Halide Perovskites. *Annu. Rev. Phys. Chem.* **2016**, *67* (1), 65–89.

(12) Leijtens, T.; Eperon, G. E.; Barker, A. J.; Grancini, G.; Zhang, W.; Ball, J. M.; Kandada, A. R. S.; Snaith, H. J.; Petrozza, A. Carrier Trapping and Recombination: The Role of Defect Physics in Enhancing the Open Circuit Voltage of Metal Halide Perovskite Solar Cells. *Energy Environ. Sci.* **2016**, *9* (11), 3472–3481.

(13) Chen, Y.; Yi, H.-T.; Wu, X.; Haroldson, R.; Gartstein, Y. N.; Rodionov, Y. I.; Tikhonov, K. S.; Zakhidov, A.; Zhu, X.-Y.; Podzorov, V. Extended Carrier Lifetimes and Diffusion in Hybrid Perovskites Revealed by Hall Effect and Photoconductivity Measurements. *Nat. Commun.* **2016**, *7*, 12253.

(14) Mitzi, D. B. Solution-Processed Inorganic Semiconductors. *J. Mater. Chem.* **2004**, *14* (15), 2355–2365.

(15) Frost, J. M.; Walsh, A. What Is Moving in Hybrid Halide Perovskite Solar Cells? *Acc. Chem. Res.* **2016**, *49*, 528–535.

(16) Yaffe, O.; Guo, Y.; Hull, T.; Stoumpos, C.; Tan, L. Z.; Egger, D. A.; Zheng, F.; Szpak, G.; Semonin, O. E.; Beecher, A. N.; Heinz, T. F.; Kronik, L.; Rappe, A. M.; Kanatzidis, M. G.; Owen, J. S.; Pimenta, M. A.; Brus, L. E. Local Polar Fluctuations in Lead Halide Perovskite Crystals. *Phys. Rev. Lett.* **2017**, *118*, 136001.

(17) Quarti, C.; Mosconi, E.; De Angelis, F. Interplay of Orientational Order and Electronic Structure in Methylammonium Lead Iodide: Implications for Solar Cell Operation. *Chem. Mater.* **2014**, *26* (22), 6557–6569.

(18) Berdiyorov, G. R.; Kachmar, A.; El-mellouhi, F.; Carignano, M. A.; Madjet, M. E.-A. Role of Cations on the Electronic Transport and Optical Properties of Lead-Iodide Perovskites. *J. Phys. Chem. C* **2016**, *120*, 16259–16270.

(19) Takabatake, T.; Suekuni, K.; Nakayama, T.; Kaneshita, E. Phonon-Glass Electron-Crystal Thermoelectric Clathrates: Experiments and Theory. *Rev. Mod. Phys.* **2014**, *86* (2), 669.

(20) Wasylishen, R. E.; Knop, O.; Macdonald, J. B. Cation Rotation in Methylammonium Lead Halides. *Solid State Commun.* **1985**, *56* (7), 581–582.

(21) Onoda-Yamamuro, N.; Matsuo, T.; Suga, H. Dielectric Study of CH3NH3PbX3 (X = Cl, Br, I). *J. Phys. Chem. Solids* **1992**, *53* (7), 935–939.

(22) Létoublon, A.; Paofai, S.; Rufflé, B.; Bourges, P.; Hehlen, B.; Michel, T.; Ecolivet, C.; Durand, O.; Cordier, S.; Katan, C.; Even, J. Elastic Constants, Optical Phonons, and Molecular Relaxations in the High Temperature Plastic Phase of the CH3NH3PbBr3 Hybrid Perovskite. *J. Phys. Chem. Lett.* **2016**, *7* (19), 3776–3784.

(23) Mashiyama, H.; Kurihara, Y. Disordered Cubic Perovskite Structure of CH3NH3PbX3 (X = Cl , Br , I). *Phys. B* **1998**, *32*, 156–158.

(24) Chen, T.; Foley, B. J.; Ipek, B.; Tyagi, M.; Copley, J. R. D.; Brown, C. M.; Choi, J. J.; Lee, S.-H. Rotational Dynamics of Organic Cations in CH3NH3PbI3 Perovskite. **2015**.

(25) Swainson, I. P.; Stock, C.; Parker, S. F.; Van Eijck, L.; Russina, M.; Taylor, J. W. From Soft Harmonic Phonons to Fast Relaxational Dynamics in CH3NH3PbBr3. *Phys. Rev. B*

2015, *92* (10), 100303.

(26) Beecher, A. N.; Semonin, O. E.; Skelton, J. M.; Frost, J. M.; Terban, M. W.; Zhai, H.; Alatas, A.; Owen, J. S.; Walsh, A.; Billinge, S. J. L. Direct Observation of Dynamic Symmetry Breaking above Room Temperature in Methylammonium Lead Iodide Perovskite. *ACS Energy Lett.* **2016**, *1*, 880–887.

(27) Sendner, M.; Nayak, P. K.; Egger, D. A.; Beck, S.; Müller, C.; Epding, B.; Kowalsky, W.; Kronik, L.; Snaith, H. J.; Pucci, A.; Lovrinči, R. Optical Phonons in Methylammonium Lead Halide Perovskites and Implications for Charge Transport. *Mater. Horizons* **2016**, *3*, 1–8.

(28) Leguy, A. M. A.; Goñi, A. R.; Frost, J. M.; Skelton, J.; Brivio, F.; Rodríguez-Martínez, X.; Weber, O. J.; Pallipurath, A.; Alonso, M. I.; Campoy-Quiles, M.; Weller, M. T.; Nelson, J.; Walsh, A.; Barnes, P. R. F. Dynamic Disorder, Phonon Lifetimes, and the Assignment of Modes to the Vibrational Spectra of Methylammonium Lead Halide Perovskites. *Phys. Chem. Chem. Phys.* **2016**, *18*, 27051–27066.

(29) Zhu, H.; Miyata, K.; Fu, Y.; Wang, J.; Joshi, P.; Niesner, D.; Williams, K. W.; Jin, S.; Zhu, X.-Y. Screening in Crystalline Liquids Protects Energetic Carriers in Hybrid Perovskites. *Science* **2016**, *353* (6306), 1409–1413.

(30) Weller, M. T.; Weber, O. J.; Henry, P. F.; Di Pumpo, A. M.; Hansen, T. C. Complete Structure and Cation Orientation in the Perovskite Photovoltaic Methylammonium Lead Iodide between 100 and 352 K. *Chem. Commun.* **2015**, *51*, 4180–4183.

(31) Miyata, K.; Meggiolaro, D.; Trinh, M. T.; Joshi, P. P.; Mosconi, E.; Jones, S. C.; De Angelis, F.; Zhu, X. Large Polarons in Lead Halide Perovskites. *Sci. Adv.* **2017**, *3*, e1701217.

(32) Rakita, Y.; Cohen, S. R.; Kedem, N. K.; Hodes, G.; Cahen, D. Mechanical Properties of APbX3 (A=Cs or CH3NH3; X=I or Br) Perovskite Single Crystals. *MRS Commun.* **2015**, *5* (4), 623–629.

(33) Fröhlich, H. Electrons in Lattice Fields. *Adv. Phys.* **1954**, *3* (11), 325–361.

(34) Emin, D. *Polarons*; Cambridge University Press: Cambridge, 2013.

(35) Feynman, R. P. Slow Electrons in a Polar Crystal. *Phys. Rev.* **1955**, *97* (3), 660.

(36) Monahan, D. M.; Guo, L.; Lin, J.; Dou, L.; Yang, P.; Fleming, G. R. A Room Temperature Coherent Optical Phonon in 2D Electronic Spectra of CH3NH3PbI3 Perovskite Is a Possible Cooling Bottleneck. *J. Phys. Chem. Lett.* **2017**, *8*, 3211–3215.

(37) Kim, H.; Cánovas, E.; Karakus, M.; Mics, Z.; Grechko, M.; Turchinovich, D.; Parekh, S. H.; Hunger, J.; Bonn, M. Coherent Phonon-Induced Modulation of the Optical Band Gap in Methylammonium Lead Halide Perovskites. *Nat. Commun.* **2017**, in press.

(38) Zhu, X.; Podzorov, V. Charge Carriers in Hybrid Organic-Inorganic Lead Halide Perovskites Might Be Protected as Large Polarons. *J. Phys. Chem. Lett.* **2015**, *23* (0), 1–16.

(39) Miyano, K.; Tripathi, N.; Yanagida, M.; Shirai, Y. Lead Halide Perovskite Photovoltaic as a Model P − I − N Diode. *Acc. Chem. Res.* **2016**, *49*, 303–310.

(40) Walsh, A.; Scanlon, D. O.; Chen, S.; Gong, X. G.; Wei, S. H. Self-Regulation Mechanism for Charged Point Defects in Hybrid Halide Perovskites. *Angew. Chemie - Int. Ed.* **2015**, *54* (6), 1791–1794.

(41) Yin, W.-J.; Shi, T.; Yan, Y. Unusual Defect Physics in CH3NH3PbI3 Perovskite Solar Cell Absorber. *Appl. Phys. Lett.* **2014**, *104* (6), 63903.

(42) Niesner, D.; Zhu, H.; Miyata, K.; Joshi, P. P.; Evans, T. J. S.; Kudisch, B. J.; Trinh, M. T.; Marks, M.; Zhu, X. Persistent Energetic Electrons in Methylammonium Lead Iodide Perovskite Thin Films. *J. Am. Chem. Soc.* **2016**, *138*, 15717–15726.

(43) Brivio, F.; Butler, K. T.; Walsh, A.; Van Schilfgaarde, M. Relativistic Quasiparticle Self-Consistent Electronic Structure of Hybrid Halide Perovskite Photovoltaic Absorbers. *Phys. Rev. B - Condens. Matter Mater. Phys.* **2014**, *89* (15), 155204.

(44) Yin, W.-J.; Yang, J.-H.; Kang, J.; Yan, Y.; Wei, S.-H. Halide Perovskite Materials for Solar Cells: A Theoretical Review. *J. Mater. Chem. A* **2015**, *0*, 1–17.

(45) Umari, P.; Mosconi, E.; De Angelis, F. Relativistic GW Calculations on CH3NH3PbI3 and CH3NH3SnI3 Perovskites for Solar Cell Applications. *Sci. Rep.* **2014**, *4*, 4467.

(46) Herz, L. M. Charge-Carrier Mobilities in Metal Halide Perovskites: Fundamental Mechanisms and Limits. *ACS Energy Lett.* **2017**, 1539–1548.

(47) Saidaminov, M. I.; Abdelhady, A. L.; Murali, B.; Alarousu, E.; Burlakov, V. M.; Peng, W.; Dursun, I.; Wang, L.; He, Y.; Maculan, G.; Goriely, A.; Wu, T.; Mohammed, O. F.; Bakr, O. M. High-Quality Bulk Hybrid Perovskite Single Crystals within Minutes by Inverse Temperature Crystallization. *Nat. Commun.* **2015**, *6* (May), 7586.

(48) Yi, H. T.; Wu, X.; Zhu, X.-Y.; Podzorov, V. Intrinsic Charge Transport across Phase Transitions in Hybrid Organo-Inorganic Perovskites. *Adv. Mater.* **2016**, *28* (30), 6509–6514.

(49) Feynman, R. P.; Hellwarth, R. W.; Iddings, C. K.; Platzman, P. M. Mobility of Slow Electrons in a Polar Crystal. *Phys. Rev.* **1962**, *127* (4), 1004–1017.

(50) Osaka, Y. Polaron State at a Finite Temperature. *Prog. Theor. Phys.* **1959**, *22* (3), 437–446.

(51) Hendry, E.; Wang, F.; Shan, J.; Heinz, T. F.; Bonn, M. Electron Transport in TiO2 Probed by THz Time-Domain Spectroscopy. *Phys. Rev. B* **2004**, *69* (8), 81101.

(52) Hellwarth, R. W.; Biaggio, I. Mobility of an Electron in a Multimode Polar Lattice. *Phys. Rev. B* **1999**, *60* (1), 299.

(53) Milot, R. L.; Eperon, G. E.; Snaith, H. J.; Johnston, M. B.; Herz, L. M. Temperature-Dependent Charge-Carrier Dynamics in CH3NH3PbI3 Perovskite Thin Films. *Adv. Funct. Mater.* **2015**, *25* (39), 6218–6227.

(54) Savenije, T. J.; Ponseca, C. S.; Kunneman, L.; Abdellah, M.; Zheng, K.; Tian, Y.; Zhu, Q.; Canton, S. E.; Scheblykin, I. G.; Pullerits, T.; Yartsev, A.; Sundström, V. Thermally Activated Exciton Dissociation and Recombination Control the Carrier Dynamics in Organometal Halide Perovskite. *J. Phys. Chem. Lett.* **2014**, *5* (13), 2189–2194.

(55) Karakus, M.; Jensen, S. A.; D'Angelo, F.; Turchinovich, D.; Bonn, M.; Cánovas, E.

Phonon-Electron Scattering Limits Free Charge Mobility in Methylammonium Lead Iodide Perovskites. *J. Phys. Chem. Lett.* **2015**, *6* (24), 4991–4996.

(56) Oga, H.; Saeki, A.; Ogomi, Y.; Hayase, S.; Seki, S. Improved Understanding of the Electronic and Energetic Landscapes of Perovskite Solar Cells : High Local Charge Carrier Mobility , Reduced Recombination , and Extremely Shallow Traps. *J. Am. Chem. Soc.* **2014**, *136*, 13818–13825.

(57) Bardeen, J.; Shockley, W. Deformation Potentials and Mobilities in Non-Polar Crystals. *Phys. Rev.* **1950**, *80* (1), 72–80.

(58) He, Y.; Galli, G. Perovskites for Solar Thermoelectric Applications: A First Principle Study of CH3NH3AI3 (A = Pb and Sn). *Chem. Mater.* **2014**, *26* (18), 5394–5400.

(59) Zhao, T.; Shi, W.; Xi, J.; Wang, D.; Shuai, Z. Intrinsic and Extrinsic Charge Transport in CH3NH3PbI3 Perovskites Predicted from First-Principles. *Sci. Rep.* **2016**, *7*.

(60) Wang, Y.; Zhang, Y.; Zhang, P.; Zhang, W. High Intrinsic Carrier Mobility and Photon Absorption in the Perovskite CH3NH3PbI3. *Phys. Chem. Chem. Phys.* **2015**, *17* (17), 11516–11520.

(61) Mante, P.-A.; Stoumpos, C. C.; Kanatzidis, M. G.; Yartsev, A. Electron–acoustic Phonon Coupling in Single Crystal CH3NH3PbI3 Perovskites Revealed by Coherent Acoustic Phonons. *Nat. Commun.* **2017**, *8*, 14398.

(62) Filippetti, A.; Mattoni, A.; Caddeo, C.; Saba, M. I.; Delugas, P. Low Electron-Polar Optical Phonon Scattering at the Fundament of Carrier Mobility in Methylammonium Lead Halide CH3NH3PbI3 Perovskites. *Phys. Chem. Chem. Phys.* **2016**, *18*, 15352–15362.

(63) Wehrenfennig, C.; Eperon, G. E.; Johnston, M. B.; Snaith, H. J.; Herz, L. M. High Charge Carrier Mobilities and Lifetimes in Organolead Trihalide Perovskites. *Adv. Mater.* **2014**, *26* (10), 1584–1589.

(64) Wright, A. D.; Verdi, C.; Milot, R. L.; Eperon, G. E.; Pérez-Osorio, M. A.; Snaith, H. J.; Giustino, F.; Johnston, M. B.; Herz, L. M. Electron–phonon Coupling in Hybrid Lead Halide Perovskites. *Nat. Commun.* **2016**, *7* (May), 11755.

(65) Frost, J. M. Calculating Polaron Mobility in Halide Perovskites. **2017**.

(66) Even, J.; Pedesseau, L.; Katan, C. Analysis of Multivalley and Multibandgap Absorption and Enhancement of Free Carriers Related to Exciton Screening in Hybrid Perovskites. *J. Phys. Chem. C* **2014**, *118* (22), 11566–11572.

(67) Anusca, I.; Balčiūnas, S.; Gemeiner, P.; Svirskas, Š.; Sanlialp, M.; Lackner, G.; Fettkenhauer, C.; Belovickis, J.; Samulionis, V.; Ivanov, M.; Dkhil, B.; Banys, J.; Shvartsman, V. V.; Lupascu, D. C. Dielectric Response: Answer to Many Questions in the Methylammonium Lead Halide Solar Cell Absorbers. *Adv. Energy Mater.* **2017**, *7*, 1700600.

(68) Cohen, M.; Chelikowsky, J. R. *Electronic Structure and Optical Properties of Semiconductors*; Springer Science & Business Media, 2012; Vol. 75.

(69) Hata, T.; Giorgi, G.; Yamashita, K. The Effects of the Organic-Inorganic Interactions on

the Thermal Transport Properties of CH3NH3PbI3. *Nano Lett.* **2016**, *16* (4), 2749–2753.

(70) Miyata, K.; Atallah, T. L.; Zhu, X. -Y. Lead Halide Perovskites: Crystal-Liquid Duality, Phonon Glass Electron Crystals, and Large Polaron Formation. *Sci. Adv.* **2017**.

(71) Hubbard, J. B.; Onsager, L. Dielectric Dispersion and Dielectric Friction in Electrolyte Solutions. I. *J. Chem. Phys.* **1977**, *67* (1977), 4850.

(72) Zwanzig, R. Dielectric Friction on a Rotating Dipole. *J. Chem. Phys.* **1963**, *38* (7), 1605.

(73) Heitele, H. Dynamic Solvent Effects on Electron-Transfer Reactions. *Angew. Chemie Int. Ed. English* **1993**, *32* (3), 359–377.

(74) Bakulin, A.; Selig, O.; Bakker, H. J.; Rezus, Y. L. a.; Müller, C.; Glaser, T.; Lovrincic, R.; Sun, Z.; Chen, Z.; Walsh, A.; Frost, J. M.; Jansen, T. L. C. Real-Time Observation of Organic Cation Reorientation in Methylammonium Lead Iodide Perovskites. *J. Phys. Chem. Lett.* **2015**, *6* (8), 3663–3669.

(75) Tielrooij, K. J.; Petersen, C.; Rezus, Y. L. A.; Bakker, H. J. Reorientation of HDO in Liquid H2O at Different Temperatures: Comparison of First and Second Order Correlation Functions. *Chem. Phys. Lett.* **2009**, *471* (1), 71–74.

(76) Fried, L. E.; Mukamel, S. Solvation Structure and the Time-Reslved Stokes Shift in Non-Debye Solvent. *J. Chem. Phys.* **1990**, *93*, 932.

(77) Castner, E. W.; Fleming, G. R.; Bagchi, B.; Maroncelli, M. The Dynamics of Polar Solvation: Inhomogeneous Dielectric Continuum Models. *J. Chem. Phys.* **1988**, *89* (6), 3519–3534.

(78) Maroncelli, M.; Kumar, V. P.; Papazyan, A. A Simple Interpretation of Polar Solvation Dynamics. *J. Phys. Chem.* **1993**, *97* (1), 13–17.

(79) Ma, J.; Wang, L. W. Nanoscale Charge Localization Induced by Random Orientations of Organic Molecules in Hybrid Perovskite CH3NH3PbI3. *Nano Lett.* **2015**, *15* (1), 248–253.

(80) Ma, J.; Wang, L.-W. The Nature of Electron Mobility in Hybrid Perovskite CH3NH3PbI3. *Nano Lett.* **2017**, *17* (6), 3646–3654.